Structure and morphology of thin MgO films on Mo(001)

S. Benedetti, P. Torelli, and S. Valeri
Dipartimento di Fisica and CNR-INFM National Research Center on nanoStructures and bioSystems at Surfaces (S3), Università di Modena e Reggio Emilia, Via G. Campi 213/a, I-41100 Modena, Italy

H. M. Benia and N. Nilius
Fritz-Haber-Institut der Max-Planck-Gesellschaft, Faradayweg 4-6, D-14195 Berlin, Germany

G. Renaud
CEA, Inac, SP2M, NRS, F-38054 Grenoble Cedex, France

(Received 19 June 2008; revised manuscript received 15 October 2008; published 11 November 2008)

Using a combination of reciprocal and real-space techniques, the structural evolution and its effect on the surface morphology is investigated for MgO films of 1–30 ML thickness epitaxially grown on Mo(001). The strain induced by the mismatch with the substrate is relieved between 1 and 7 ML MgO due to the formation of an ordered network of interfacial misfit dislocations aligned along the MgO ⟨110⟩ directions, particularly evident after annealing the film at 1070 K. A dislocation periodicity of about 60 Å has been determined by means of grazing incidence x-ray diffraction. The dislocations induce a tilting of the surface that appears in electron diffraction along the ⟨100⟩ MgO directions for thin films and changes to ⟨110⟩ directions when the oxide thickness increases. Scanning tunneling microscopy (STM) shows the presence of a regular pattern on the surface below 7 ML thickness associated to the dislocation network. With increasing thickness, screw dislocations connected by nonpolar steps appear on the oxide surface. Thanks to the combination of different diffraction techniques and STM measurements, a comprehensive picture of the relaxation mechanisms in MgO films on Mo(001) can be drawn.

DOI: 10.1103/PhysRevB.78.195411 PACS number(s): 68.55.−a, 68.47.Gh, 68.35.−p

I. INTRODUCTION

Strain relaxation is a fundamental issue to determine the structural and morphological stabilities of lattice-mismatched epitaxial systems. For semiconductor or metal heteroepitaxy with a lattice mismatch with the substrate $m<10\%$ [defined as $m=(a_f-a_s)/a_s$, with a_f and a_s being the film and substrate lattice parameters, respectively], overlayers relax the misfit strain in different ways once a certain critical thickness is exceeded. Typically relaxation occurs by (i) formation of dislocation-free islands on top of a wetting layer (or Stranski-Krastanov growth mode), typical for semiconductor heteroepitaxy;[1] or (ii) insertion of misfit dislocations in the film or islands.[2] These processes depend on the balance of various energetic terms, such as surface and interface energies, the energy cost for dislocation formation, as well as on kinetic limitations. These mechanisms have been investigated extensively for semiconductors and metals, while few works give detailed insights into the relaxation of thin oxide films grown on metallic surfaces.[3,4]

MgO is a suitable model oxide to study strain relief because of its stable and inert character and its simple rocksalt structure. In addition, MgO thin films are used as support in heterogeneous catalysis and in magnetoelectronic devices, and a good understanding of their relaxation behavior is therefore required to improve such applications.[5–7] For this reason, MgO has been prepared and investigated in the form of thin films on a variety of metal substrates, such as Ag(001),[8–10] Fe(001),[11,12] and Mo(001).[13,14] Particularly interesting is the use of Mo(001) because of its high thermal stability and the relatively small mismatch of −5.2% with bulk MgO that allows an epitaxial growth with the relationship MgO(001)//Mo(001) and MgO[110]//Mo[100]. In a recent work we have studied the morphology of MgO thin films deposited on Mo(001), where after annealing at 1070 K a flat and well-ordered surface is produced.[15] For low oxide thickness we observed the formation of a square network with a periodicity of about 55 Å and a [110] orientation in the scanning tunneling microscopy (STM), while low-energy electron diffraction (LEED) revealed the presence of surface regions with a tilt along the [100] direction with respect to the (001) plane. Similar networks have been observed on other rocksalt systems by means of STM and x-ray scattering, not only on metal-oxide systems[16,17] but also on semiconductors.[18] Those experiments demonstrated the close connection between relaxation processes in the film material and the formation of defect networks. The CoO/Ag(001) system exhibits a [110] dislocation network in x-ray diffraction.[16] For MgO on Fe(001) and Ag(001), the appearance of a surface tilting in LEED parallel to the [100] direction is attributed to the formation of [100] dislocations by the glide system $\frac{1}{2}$[110](110).[3,4,12] The long-range order of the dislocation network is, however, not discussed in those papers. Additionally the lattice mismatch with the MgO is rather small for substrates such as Ag (−3.2%) and Fe (+3.8%), compared to the present case. Only for NiO/Pd(001), both the square network and the tilting have been observed.[19] While the first has been tentatively assigned to Moiré-type interference or to an ordered dislocation network, the latter has been related to the alignment of island borders.

This work aims for a detailed study of the structural evolution of the MgO/Mo system by means of diffraction techniques and STM to precisely determine the nature and orientation of interfacial misfit dislocations in MgO and its

relation with the surface deformation as a function of thickness. As Mo as refractory metal withstands high temperatures, the effect of a thorough annealing on the morphology of the metal-oxide system is investigated too. The application of complementary techniques and different sample preparations allow us to propose a detailed and comprehensive model of the relaxation mechanisms in MgO thin films.

II. EXPERIMENTAL

The structure of the MgO/Mo(001) system has been investigated by means of grazing incidence x-ray diffraction (GIXD), LEED, and primary-beam diffraction modulated electron emission (PDMEE). GIXD measurements have been performed at ESRF in Grenoble at the beamline BM32,[20] using a photon energy of 18 keV. The fixed incidence angle, $\alpha_i = 0.166°$, was chosen below the critical angle for total external reflection in Mo (0.19°) but above that of MgO (0.12°). The GIXD scans shown in this paper are represented in reciprocal-lattice unit (rlu) scale for h, k, and l of the reciprocal Mo(001) lattice, where the lattice parameter is $a = 3.147$ Å. The l coordinate is perpendicular to the MgO/Mo(001) interface.

LEED analysis was performed using a three-grid apparatus and the diffraction patterns were recorded by a charge-coupled device (CCD) camera. PDMEE measurements were performed at the SESAMO laboratory in Modena in an UHV chamber with a cylindrical mirror analyzer operating in the first derivative mode (0.6% resolution, 15 eV modulation) and a coaxial electron gun working at 5 keV and $1-2$ μA.[21]

STM measurements were carried out at the Fritz-Haber-Institut in Berlin with a beetle-type STM operated at liquid-nitrogen temperature (70 K) and ultra-high-vacuum conditions ($p \sim 5 \times 10^{-10}$ mbar).

The Mo substrate was prepared either by sputtering at 1170 K (Ar^+, 600 eV) or by flashing at 2300 K because of the different possibilities in the used machines. The MgO film was grown by reactive deposition of Mg in O_2 partial pressure of 1×10^{-7} mbar, keeping the substrate at room temperature (MgO deposition rate = 1.22 ML/min). After the deposition the samples were annealed at 1070 K for 10 min.

Film thickness in this paper has been estimated by means of a quartz microbalance and x-ray photoelectron spectroscopy (XPS). In a previous paper, measurements by STM on the same system underestimated the thickness by a factor of 2.[15]

III. RESULTS AND DISCUSSION

A. Film relaxation

The structural relaxation of the MgO film has been studied combining different techniques to determine both the evolution of in-plane and out-of-plane lattice parameters. In-plane parameters have been determined by GIXD. In the GIXD measurements, two components in the Mo peak are recognizable that are assigned to the presence of grains in the metal substrate. Due to the preparation via high-temperature sputtering, the grain structure and therefore the shape of the Mo peak slightly vary for different experimental runs. Figure 1(a) shows the evolution of $(h,0,0.03)$ scan along the (200) Mo Bragg peak for increasing MgO thickness. Besides the Mo peak at $h=2$ rlu, for 2 ML deposit a shoulder appears at about $h=2.05$ rlu that is assigned to the MgO Bragg peak. The shoulder evolves to a well defined peak that moves to a larger h value up to 2.11 rlu for 25 ML thick films, indicating the in-plane relaxation of MgO. The in-plane lattice parameter of the oxide film is obtained from the reciprocal space position of the peaks in Fig. 1(a) fitted with a set of Gaussian peaks and it is reported in Fig. 1(b) (empty dots). The film starts relaxing at 2 ML, but even at 25 ML it is not fully relaxed and 0.5% of the strain remains [the strain is defined here as $S=(d_{\parallel}-d_0)/d_0$, where $d_{\parallel}, d_0$ are the in-plane and the bulk Mg-O distances, respectively]. This is due to the finite film thickness that prevents complete relaxation. The effect of film annealing on the release of the strain has also been studied and the evolution of the in-plane parameter as a function of thickness in annealed films is reported in Fig. 1(b) (solid markers). After thermal treatment at 1070 K the 1 ML film has decreased its strain from 5.5% to 1.5%, a process that is nearly saturated already at 7 ML thickness.

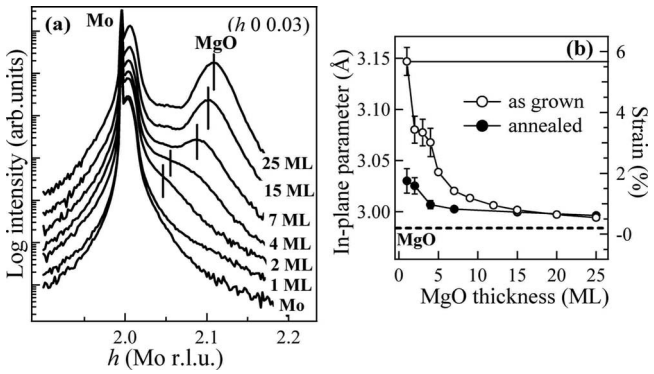

FIG. 1. (a) Radial scans along the $(h,0,0.03)$ direction around the (200) Mo Bragg peak for as-grown MgO film of increasing thickness. Curves have been vertically shifted for clarity. (b) Evolution of the in-plane MgO parameter, along the MgO[110] direction, as a function of film thickness before (○) and after annealing at 1070 K (●).

The out-of-plane lattice parameter has been determined with PDMEE. PDMEE plots are reported in Fig. 2(a), where the intensity angular distribution (IAD) of the O and Mg KLL Auger signals as a function of incidence angle along the [100] Mo azimuth are shown for 2–28 ML thick MgO films after annealing, together with the Mo MNN IAD of the clean substrate. The main features of the rocksalt (001) structure are evident and rationalized by the model structure in the inset. Forward focusing peaks occur at 0° and 55° for MgO, corresponding to the primary beam alignment along the [001] and [111] atomic chains, respectively. Other features are mainly generated by higher order interference and cannot directly be related to specific atomic alignments, though characteristic of the MgO structure, as deduced from the IAD of a bulk MgO. On the other hand, Mo MNN IAD shows main features at 0° and 45°, corresponding to the alignment along the [001] and [101] atomic chains of a bcc (001) crystal rotated in plane by 45° with respect to the MgO structure. This confirms the expected epitaxial growth, with the MgO [110] direction aligned to the Mo[100] one.

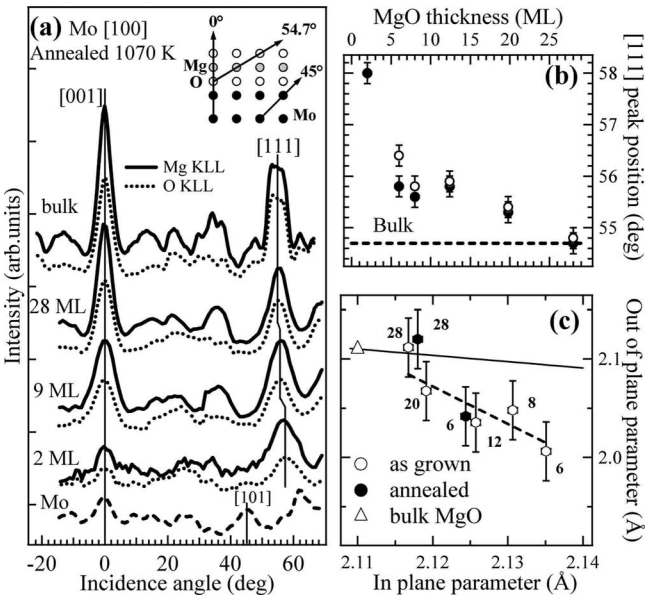

FIG. 2. (a) IADs of Mg KLL (solid line) and O KLL (dotted line) Auger signals along the [100] Mo azimuth for 2–28 ML MgO after annealing at 1070 K. IADs of bulk MgO (top curves) and the Mo MNN IAD of the clean substrate (dashed line) are shown for comparison. Each plot has been scaled to its 0° peak anisotropy. Inset: side view of the rocksalt MgO on the bcc Mo structure cut along the Mo [100]. (b) Angular position of the [111] peak of Mg KLL IAD along the [100]Mo azimuth as a function of MgO thickness for the as-grown (○) and annealed (●) samples. (c) Out-of-plane Mg-O distance as a function of in-plane distance obtained by PDMEE and GIXD analysis, respectively. The values for a bulk MgO are shown with an open triangle. The solid line represents the values calculated with the MgO bulk elastic constants (γ=0.64, see text for details), while the dashed line indicates the best fit of the experimental data for as-grown (○) films (γ=3.8). Numbers next to each point indicate the corresponding MgO thickness in ML.

The IADs at low thickness are characterized by the [111] peak shifted to higher angles, indicating a tetragonal distortion of the MgO film as induced by the larger in-plane lattice parameter of the substrate. With relaxation of the strain at increasing thickness, the peak moves toward its bulk position. In Fig. 2(b), the angular position of the [111] peak is reported as a function of film thickness for both the as-grown and the annealed films. The peak position changes not only with increasing thickness but also with annealing, suggesting that the thermal treatment improves the crystal quality and accelerates film relaxation, as already revealed from the GIXD data [Fig. 1(b)].

Out-of-plane parameter $d_\perp$ has been extracted combining the angular position ϑ of the [111] peak obtained by PDMEE and the in-plane parameter $d_\parallel$ from GIXD, given that $\tan\vartheta = d_\parallel/d_\perp$. The Mg-O distances are summarized in Fig. 2(c) as a function of the in-plane value. The solid line describes the expected behavior from the elastic theory approximation,[22] according to the equation,

$$d_\perp = -\gamma d_\parallel + (1+\gamma)d_0, \tag{1}$$

where γ is defined as $\gamma = 2C_{12}/C_{11}$, with C_{11} and C_{12} as the elastic stiffness constants of bulk MgO.[23] The open triangle

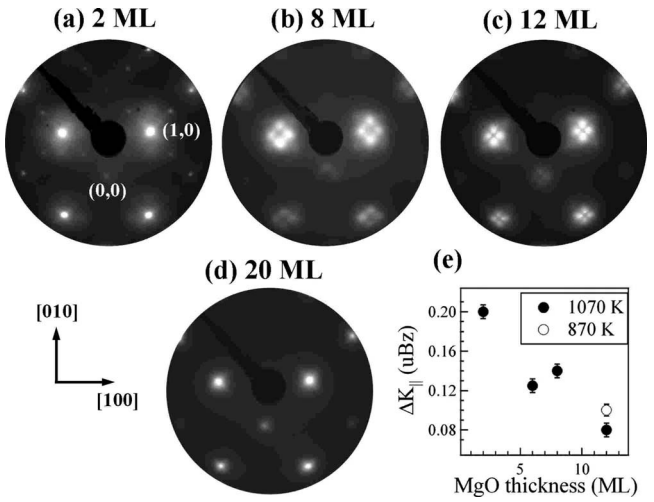

FIG. 3. LEED pattern for (a) 2, (b) 8, (c) 12, (d) 20 ML MgO on Mo(001), and (e) spot splitting in units of the first Brillouin zone (uBz) as a function of MgO thickness after annealing at 1070 K (●) and for 12 ML after annealing at 870 K (○) (E_p=100 eV).

represents the unstrained bulk MgO $d_\perp = d_\parallel = d_0 = 2.11$ Å, while $d_\parallel = 2.23$ Å and $d_\perp = 2.04$ Å would be expected in case of perfect pseudomorphism. If we fit the experimental data for the as-grown film with Eq. (1), we obtain a γ value of 3.8, larger than the value of 0.64 obtained on a bulk MgO. We therefore conclude that the film elastic behavior does not correspond to the bulk one, in contrast to the behavior of NiO and MgO films on Ag(001).[24,25] In the present case, the out-of-plane compression is larger than expected, suggesting a variation in the elastic properties of the MgO film. This can be ascribed to the large negative mismatch with the Mo substrate that induces a strong MgO deformation. The subsequent formation of interfacial dislocations modifies the relaxation characteristics, as shown below. In addition, Mo in contrast to Ag does not accommodate misfit itself because of its larger hardness and its bcc crystal structure as compared to rocksalt MgO and fcc Ag.

B. Surface deformation

During the relaxation of the film, a surface deformation becomes evident in the MgO/Mo system. LEED spots are in fact characterized by a fourfold splitting along the ⟨100⟩ MgO directions [Figs. 3(a)–3(c)] that depends linearly on the scattering vector. This is compatible with the formation of tilted regions on the surface, as it was shown in a previous work.[15] The spot splitting is shown in Fig. 3(e) as a function of thickness and temperature. The splitting decreases with increasing thickness and temperature, indicating the progressive flattening of the tilted surface areas due to relaxation, in accordance with the observations on MgO/Fe(001) and MgO/Ag(001).[3,4] Furthermore, with increasing thickness an additional broadening appears along the ⟨110⟩ MgO directions, particularly evident above 10 ML thickness [Fig. 3(c)]. This broadening is linearly dependent on the scattering vector and therefore related to an additional tilt rotated by 45° with respect to the low-thickness behavior. However, as the

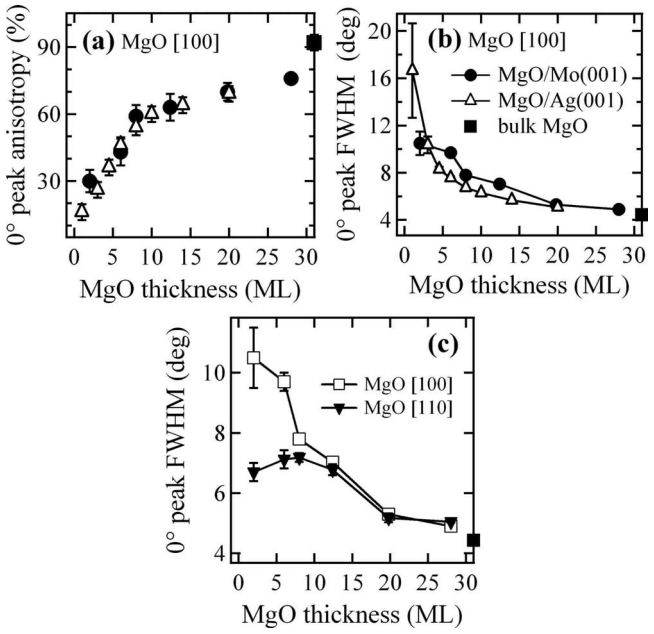

FIG. 4. (a) Anisotropy and (b) FWHM of the 0° peak of Mg KLL IAD along the [100] MgO azimuth as a function of oxide thickness in MgO/Mo(001) after annealing (●) and in MgO/Ag(001) system (△) (Ref. 26). Bulk values are reported for comparison (■). (c) FWHM of the 0° peak of Mg KLL IAD along the MgO [100] (□) and [110] azimuth (▼). Where not reported, the marker size represents the error bar on the *y* axis.

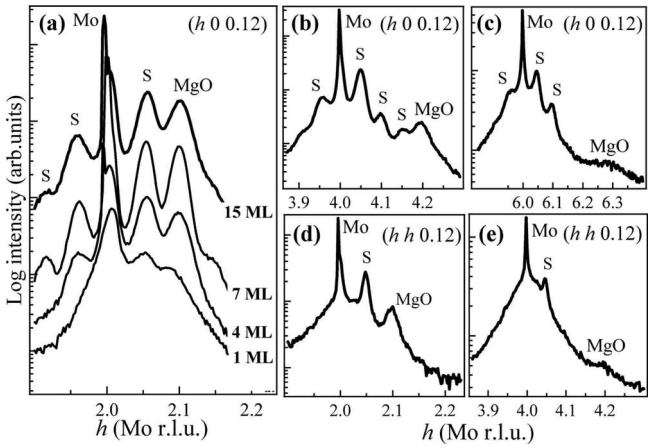

FIG. 5. (a) Radial scans along the $(h,0,0.12)$ direction around the (200) Mo Bragg peak for MgO films of increasing thickness annealed at 1070 K. [(b)–(e)] Radial scans on a 15 ML MgO film on Mo(001) annealed at 1070 K. Diffraction satellites due to the interfacial dislocation network are indicated with a "S." The *l* value of 0.12 has been chosen to maximize the satellite to bulk relative contributions.

spots are simply broad and not split into distinct satellites, it is much more difficult to assign them to a precise tilting angle. When the [100] tilt disappears above 15 ML in the LEED spots, only the [110] broadening remains visible [Fig. 3(d)].

The hypothesis of tilted surface planes is further supported by the full width at half maximum (FWHM) and the anisotropy of peaks in the PDMEE scans. The anisotropy is hereby defined as $A=2(I_{max}-I_{min})/(I_{max}+I_{min})$, with $I_{max}(I_{min})$ as the maximum (minimum) intensity of the PDMEE peak. While anisotropy increases, FWHM decreases with increasing crystal quality and thickness of the film, as more and more scatterers contribute to the signal along the surface normal (0°). An additional contribution to the FWHM possibly comes from tilted surface regions, which add components to the main peaks that are shifted by their tilting angle with respect to the normal. If the tilting angle is small and peaks are broad, the two components cannot be resolved and only a general broadening of the peak becomes visible, while the anisotropy remains unchanged. In Fig. 4, we have shown the anisotropy [Fig. 4(a)] and the FWHM [Fig. 4(b)] of the 0° peak from PDMEE scans of Mg KLL along the MgO[100] azimuth. They are compared to results taken for the MgO/Ag(001) reference system,[26] where the formation of tilted regions occurs at higher thickness, with lower average tilting angles and reduced spatial order[4] due to the smaller lattice mismatch as compared to MgO/Mo. In both systems the FWHM clearly decreases while anisotropy increases with increasing MgO thickness, indicating the expected improvement of the crystalline quality. Before annealing, the FWHM for MgO/Mo is systematically larger than for MgO/Ag and a poorer order is deduced from the peak anisotropy (not shown here). The annealing decreases the FWHM of the MgO/Mo system. However, between 2 and 10 ML the FWHM in PDMEE IADs is larger for the MgO/Mo peak than for MgO/Ag, although the 0° peak anisotropy remains comparable. The difference in the FWHM cannot therefore be explained by a reduced crystalline order but provides a hint for the presence of tilted planes. For a 6 ML MgO film on Ag the FWHM is 7.6°. If we assume this value as the value for a flat film, the measured FWHM of 10.4° for 6 ML MgO on Mo(001) can be reproduced by adding two Gaussian peaks shifted by 3° to the fundamental peak to account for tilted areas [Fig. 4(b)]. The peak broadening in the MgO/Mo system can thus be taken as evidence for the formation of tilted regions on the surface.

In addition, pronounced differences are evident in the FWHM values of the 0° peak in PDMEE scans along the MgO [100] and [110] directions [Fig. 4(c)], which are not compatible with a flat film. In particular the larger width along the [100] below 12 ML is indicative of the presence of tilted regions along that particular crystal orientations. This is in good agreement with the LEED spots, which show distinct satellites in the MgO[100] direction.

C. Misfit dislocations and morphological evolution

Annealing the MgO film at 1070 K stimulates the appearance of a satellite in GIXD scans between the (200) Mo Bragg peak and the MgO peak [Fig. 5(a)] that grows in intensity with increasing oxide thickness. This satellite is weak after room-temperature deposition [Fig. 1(a)] but becomes clear after annealing even for the 1 ML film. With increasing thickness, several orders of this satellite become visible with a relative intensity maximum at 7 ML. In fact, all radial scans show similar satellite peaks with constant periodicity

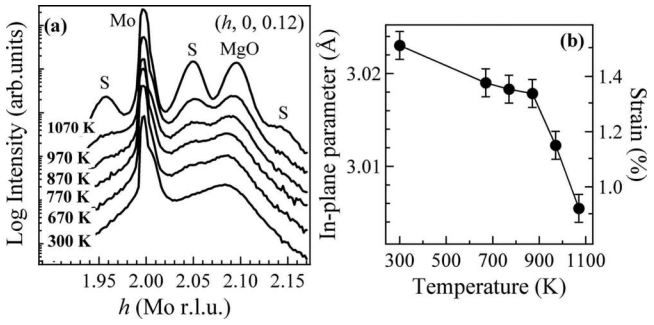

FIG. 6. (a) Radial scans along the $(h,0,0.12)$ direction around the (200) Mo Bragg peak for a 7 ML MgO film annealed at increasing temperature. (b) Evolution of the in-plane MgO lattice parameter along the Mo [100] (MgO[110]) direction as a function of annealing temperature.

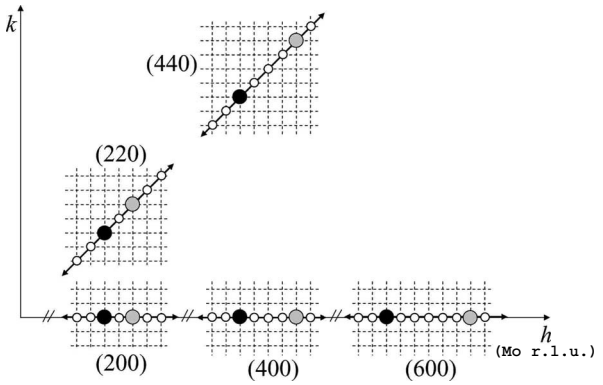

FIG. 7. Schematic representation of the $(h\ k\ 0)$ plane of the reciprocal lattice of the MgO/Mo(001) interface with an interfacial network of misfit dislocation. Black and gray dots indicate the positions of the Mo and MgO Bragg peaks, respectively. The reciprocal lattice of the dislocation network is represented with dashed lines. White dots represent the location of the satellites as expected for a [110] MgO ([100] Mo) dislocation network.

around the main Mo Bragg peaks, as shown for a 15 ML MgO film in Figs. 5(a)–5(e). This feature is assigned to the presence of a periodic network of interfacial misfit dislocations, as already reported for CoO/Ag(001) and Ag/MgO(001).[16,17] Dislocations form at 1–2 ML when the strain starts to release. However, due to an incomplete relaxation and a poor order of the dislocations at room temperature, the network is evident only after annealing the film to high temperatures. The contribution of the annealing temperature to the film relaxation is pointed out in Fig. 6, where in panel (a) $(h,0,0.12)$ radial scans of a 7 ML MgO film are depicted for increasing temperature, while in panel (b) the evolution of the in-plane lattice parameter along the MgO[110] is reported as a function of temperature. The dislocation network appears distinctly above 870 K and releases 70% of the strain left after the deposition when increasing the temperature to 1070 K.

Information on the orientation of the dislocation network can be gained by the positions of the satellite peaks. The expected satellite positions for the MgO/Mo interface in presence of a misfit dislocation network parallel to MgO ⟨110⟩ directions are illustrated by the schematic representation of the $(hk0)$ plane of the reciprocal lattice in Fig. 7. From the direct correspondence of number and positions of peaks in the measurements (Fig. 5) and in the model (Fig. 7), we can conclude that the misfit dislocations are aligned along the MgO[110] direction (equivalent to the Mo[100]). Such orientation is expected for a coincidence lattice of a rocksalt MgO and a bcc Mo rotated by 45° with respect to each other. The coincidence-site lattice is defined as the smallest superlattice formed by substrate and overlayer and represents the most probable spatial distribution of misfit dislocations. The corresponding lattice constant is given by $a_f a_s/(a_f - a_s)$, where a_f and a_s are the lattice parameter of the film and the substrate, respectively. The experimental periodicity of the dislocation network along the MgO[110] direction is determined from the positions of the GIXD satellites and was found to decrease from 68 ± 3 Å for a 2 ML film to 61 ± 1 Å for a 25 ML thick film. These values are very similar to the predictions of the coincidence lattice model [74 Å for 2 ML, 60 Å for 25 ML, using as a_f the values reported in Fig. 1(b)] and tend to the value of 56 Å, obtained from the coincidence lattice model in case of relaxed MgO on Mo.

To get a complete description of the film relaxation, we finally investigated the morphological evolution of the surface as a function of thickness with STM. Figures 8(a) and 8(b) show the surface of a 2 ML film annealed at 720 and 1070 K, respectively. In the case of mild annealing, the film is not completely closed and exhibits islands separated by holes. The resulting film roughness amounts to 1.5 nm. Annealing at high temperature provokes the coalescence of the islands and the formation of an almost continuous film with the mean roughness reduced to 0.17 nm. The film is only disrupted by a few domain boundaries with 10–20 nm separation between the original islands, as marked by the white arrow in Fig. 8(b). The growth therefore follows a perfect two-dimensional (2D) mode, as expected from the large difference in surface free energy of MgO (1.16 J/m^2) and Mo (3.87 J/m^2). In the range between 2 and 7 ML, a square pattern with a periodicity of 55 ± 5 Å and [110] orientation is observed on the surface [Fig. 8(b)], as already reported in Ref. 15. The square pattern covers the whole film, overgrowing even the domain boundaries in some cases. In some regions, the bright lines forming the square pattern end abruptly, as observable in the area marked by the rectangle in Fig. 8(b) and in the enlarged area in Fig. 8(d). The end points of the bright lines are hereby emphasized by arrows. This finding is compatible with the insertion of threading dislocations into the ordered array of misfit dislocations.

When thickness increases above 15 ML, the square pattern disappears and an almost flat surface is obtained with a mean roughness of about 0.25 nm [Fig. 8(c)]. Here screw dislocations are clearly evident [circle in Fig. 8(c)]. They are observed already in the 2 ML film, where they often form the starting point of a domain boundary [circle in Fig. 8(b)], but they reach the surface even in thicker films. In this case, the interconnection lines between two screw dislocations (the former domain boundaries) develop into steplike features and straighten along the [100] and [010] directions of MgO. The alignment of those steps results from the vanishing sta-

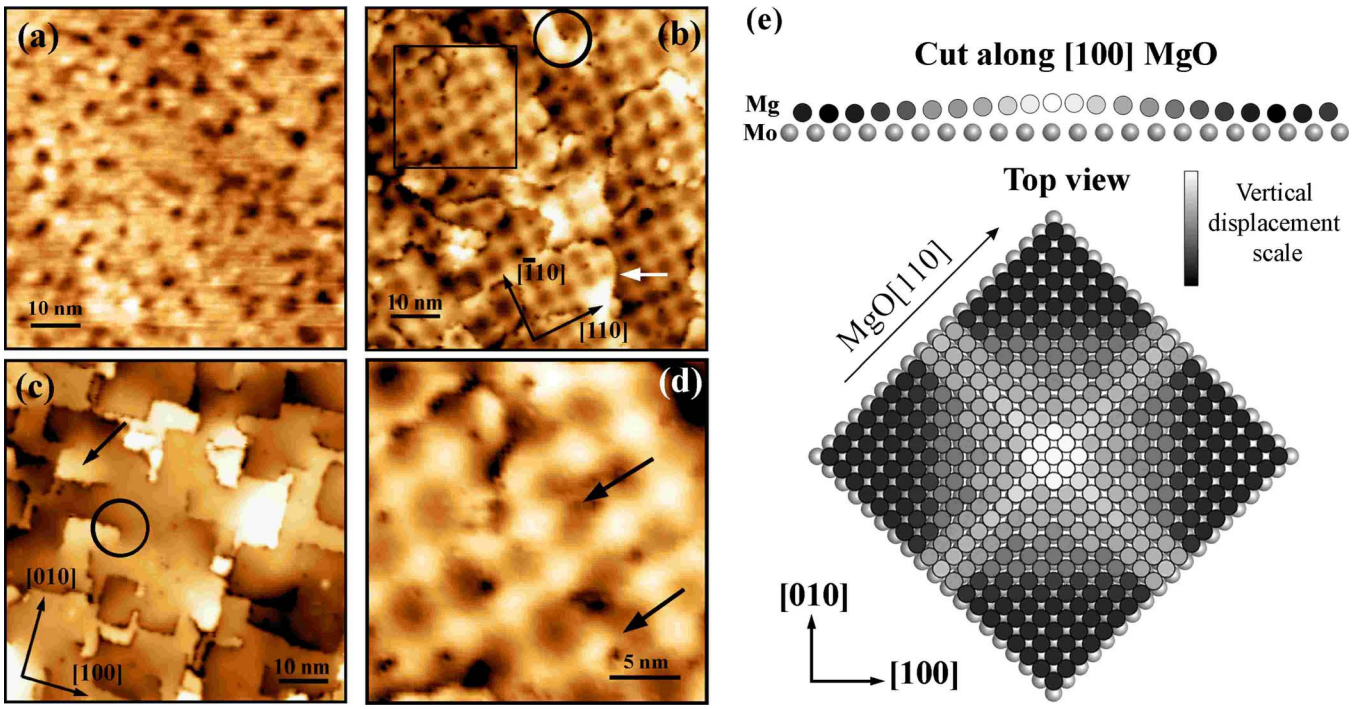

FIG. 8. (Color online) 70×70 nm^2 STM images of MgO films on Mo(001) of: (a) 2 ML annealed at 720 K (U=3.3 V); (b) 2 ML annealed at 1070 K (U=3.5 V) (white arrow indicates a domain boundary); (c) 15 ML annealed at 1070 K (U=4.8 V) (black arrow indicates a [110] tilted surface region in proximity of a screw dislocation); (d) 25×25 nm^2 zoom in of the region marked in panel (b). Black arrows indicate here the end points of two bright lines. Circles indicate examples of screw dislocations. (e) Structure model showing a cross section along the MgO[100] direction and a top view of the MgO superstructure cell. The model demonstrates the interrelation between the interfacial dislocation (gray lines) and the surface tilting. Only the Mg atoms are depicted for sake of clarity. Bright and dark areas in the model correspond to the respective regions observed in the STM images in (b) and (d).

bilization effect of polar edges by the metal support and the better crystalline order of thicker films.[27] The screw dislocations are therefore the pinning centers for the steplike features observed in Fig. 8(c). Further thickness increase leads to the development of a flat film with a reduced number of steps having exclusively ⟨100⟩ borders, while the LEED shows a simple (1×1) pattern.[15]

D. Discussion

The structural model that can be derived from the presented results is depicted in Fig. 8(e). Due to the annealing, the −5.2% lattice mismatch with the substrate rapidly relaxes in the MgO film. Between 1 and 7 ML, the main part of the misfit strain is relieved by introducing [110] misfit dislocations. Since the square pattern observed by STM in this thickness range is consistent both in size and orientation with the GIXD results, we ascribe it to the interfacial dislocation network although the underlying contrast mechanism is not clear and might be of topographic as well as of electronic origin.

The assignment of the bright lines forming the square pattern in STM to the dislocation network is also supported by the presence of threading dislocations, where the bright lines start, as seen in Fig. 8(b) and evidenced in Fig. 8(d). Because every dislocation must be terminated at the free crystal surface, there are two threading dislocations that connect each misfit dislocation with the surface layer. Starting from the interfacial layer, additional atomic planes are progressively added along the ⟨110⟩ directions with a periodicity of about 60 Å to release the strain of the MgO film. The propagation of those dislocations toward the surface produces a periodic deformation of the film, as apparent in STM images of the oxide surface. This deformation is directly related to the strain relief in the lattice-mismatched MgO/Mo system and responsible for the surface tilting with respect to the (001) plane, as revealed by the LEED satellites and the enlarged PDMEE peaks. Tilted surface planes are however not evident in STM and GIXD. The latter technique is indeed more bulk sensitive than electron diffraction, which hampers the detection of small surface perturbations such as a tilting of the surface. A tilting of roughly 5° starts to appear in the second layer and includes large portions of the surface, as the central spot in LEED is almost completely suppressed [Fig. 3(b)].[28] The tilt direction is parallel to the MgO[100] and thus rotated by 45° with respect to the dislocation lines. The driving force for the misalignment of tilting and dislocation lines might be found in the strong MgO-Mo interface interaction. As the most efficient relaxation is obtained by inserting additional atomic rows along the MgO[110] direction (the Mo[100] direction), dislocation lines might preferentially align in this particular way.

In addition, the Mo-Mg and Mo-O interactions induce a variation in the atomic out-of-plane displacement across the network. Due to the relaxation, O and Mg atoms are not always in top and hollow sites, respectively, but there are

regions of poor (areas with misfit dislocations) and good matching with the substrate atoms (in between the dislocation lines) [see Fig. 8(e)]. In the first regions, O atoms sit most probably in Mo hollow sites, while Mg are in top positions and the MgO-Mo interface distance is therefore large. In regions of good matching, O and Mg atoms are in top and hollow sites, respectively, and the film is closer to the substrate. This assumption is in accordance with theoretical predictions of a larger interfacial distance when Mg and not O atoms occupy on-top sites of the metal support.[29] Also experiments confirm that the O-top site is the most stable adsorption site on Ag substrates.[30] This vertical displacement can here be responsible for the tilted MgO planes determined from the diffraction data and shown in the model [Fig. 8(e), only Mg atoms are represented].

The ⟨100⟩ tilting is in accordance with previous observations on rocksalt oxides,[3,4,12,19] while the orientation of the dislocation network has not been clearly determined before. As LEED does not give a direct measure of the dislocation orientation, they were often assumed to be aligned along the [100] direction since no direct techniques were employed.[3,4] Only in the case of CoO/Ag, [110] oriented dislocations were directly observed by GIXD,[16] while for NiO/Pd a square [110] pattern visible in STM was tentatively assigned to interfacial dislocations.[19]

With increasing thickness, the tilting angle decreases and almost flat and fully relaxed MgO surfaces with negligible influence of the interfacial dislocation network are observed above 15 ML [Fig. 8(c)]. In this thickness regime, screw dislocations associated with monatomic nonpolar steps occur, which induce a tilting of the surface along the ⟨110⟩ directions [an example is marked by an arrow in Fig. 8(c)]. The dislocations are widely spaced (10–20 nm) and show no long-range order, in contrast to the interfacial network. As a consequence, they introduce a distribution of tilting angles and cause a starlike broadening of the LEED spots in ⟨110⟩ directions, while sharp satellites as observed for lower thickness are not observed. Following the evolution of the surface morphology, as described in Sec. III C, the monatomic steps seem to be to the evolution of the domain boundaries left by the island coalescence, which gradually align with the MgO ⟨100⟩ for increasing thickness. In this way, the screw dislocations could be related to the lateral misfit of merging oxide islands[31] or alternatively form at buried defects of the interfacial dislocation network (e.g., spiral structures nucleated on threading dislocations).[32] However, they might also be introduced in a nonregular manner into the thicker film to release the remaining misfit with the Mo support. A complete analysis of the crystallographic nature of these screw dislocations cannot be performed on the basis of the present experimental results.

Screw dislocations have never been observed before in oxide films of rocksalt structure, as the large thickness at which they occur usually prevents STM experiments. Also the resulting ⟨110⟩ tilting was not observed, with the exception of CoO/Ag(001) (Ref. 16) and NiO/Pd(001), where both ⟨100⟩ and ⟨110⟩ tilting was reported as a function of oxide thickness.[19] Comparing the different oxide systems, it becomes, however, not clear whether the relaxation follows different mechanisms in the various oxide-metal systems or the ⟨110⟩ tilting was missed due to (i) the thickness range investigated,[4,12] (ii) the low annealing temperatures, or (iii) the increased broadening of the LEED spots for thick films that prevents a detailed analysis.[3]

IV. CONCLUSIONS

To summarize, we have reported a comprehensive investigation of the structural and morphological evolution of the MgO/Mo(001) system that, thanks to the combination of real and reciprocal space techniques, leads to a complete model for the relaxation mechanism of MgO films on Mo(001). Between 1 and 7 ML the film relaxes almost completely the misfit strain by the formation of a regular array of interfacial misfit dislocations with 60 Å periodicity and MgO [110] orientation. The crucial role of high-temperature annealing for the film relaxation has clearly been demonstrated. The misfit dislocations introduce a periodic modulation of the in-plane parameter, resulting in regions of good and poor matching with the substrate lattice. The strong interaction with the Mo substrate atoms in those different regions determines the tilting of the MgO planes along the MgO[100] direction that flattens once the dislocations are buried far below the oxide surface at about 15 ML.

Between 15 and 20 ML the surface is characterized by nonpolar [100] MgO steps that could be remnants of the coalescence of MgO islands in the first stages of growth. The steps are often pinned by screw dislocations, which help releasing the remaining strain in the film and induce a surface tilting along the MgO[110] direction. Complete relaxation of MgO films on Mo(001) is not observed up to 25 ML film thickness.

ACKNOWLEDGMENT

The authors wish to acknowledge the financial support by the EU (FP6STRP "GSOMEN").

[1] Y.-W. Mo, D. E. Savage, B. S. Swartzentruber, and M. G. Lagally, Phys. Rev. Lett. **65**, 1020 (1990).

[2] J. W. Matthews and A. E. Blakeslee, J. Cryst. Growth **27**, 118 (1974).

[3] M. Dynna, J. L. Vassent, A. Marty, and B. Gilles, J. Appl. Phys. **80**, 2650 (1996).

[4] J. Wollschläger, D. Erdös, H. Goldbach, R. Höpken, and K. M. Schröder, Thin Solid Films **400**, 1 (2001).

[5] M. Sterrer, T. Risse, U. M. Pozzoni, L. Giordano, M. Heyde, H.-P. Rust, G. Pacchioni, and H.-J. Freund, Phys. Rev. Lett. **98**, 096107 (2007).

[6] G. Pacchioni, L. Giordano, and M. Baistrocchi, Phys. Rev. Lett.

94, 226104 (2005).
[7] S. Yuasa, T. Nagahame, A. Fukushima, Y. Suzuki, and K. Ando, Nature Mater. **3**, 868 (2004).
[8] S. Valeri, S. Altieri, A. di Bona, P. Luches, C. Giovanardi, and T. S. Moia, Surf. Sci. **507-510**, 311 (2002).
[9] J. Wollschläger, J. Viernow, C. Tegenkamp, D. Erdös, K. M. Schröder, and H. Pfnür, Appl. Surf. Sci. **142**, 129 (1999).
[10] S. Schintke, S. Messerli, M. Pivetta, F. Patthey, L. Libioulle, M. Stengel, A. De Vita, and W. D. Schneider, Phys. Rev. Lett. **87**, 276801 (2001).
[11] H. L. Meyerheim, R. Popescu, J. Kirschner, N. Jedrecy, M. Sauvage-Simkin, B. Heinrich, and R. Pinchaux, Phys. Rev. Lett. **87**, 076102 (2001).
[12] M. Klaua, D. Ullmann, J. Barthel, W. Wulfhekel, J. Kirschner, R. Urban, T. L. Monchesky, A. Enders, J. F. Cochran, and B. Heinrich, Phys. Rev. B **64**, 134411 (2001).
[13] M. Sterrer, E. Fischbach, T. Risse, and H.-J. Freund, Phys. Rev. Lett. **94**, 186101 (2005).
[14] M. C. Gallagher, M. S. Fyfield, L. A. Bumm, J. P. Cowin, and S. A. Joyce, Thin Solid Films **445**, 90 (2003).
[15] S. Benedetti, H. M. Benia, N. Nilius, S. Valeri, and H. J. Freund, Chem. Phys. Lett. **430**, 330 (2006).
[16] P. Torelli, E. A. Soares, G. Renaud, L. Gragnaniello, S. Valeri, X. X. Guo, and P. Luches, Phys. Rev. B **77**, 081409(R) (2008).
[17] G. Renaud, P. Guénard, and A. Barbier, Phys. Rev. B **58**, 7310 (1998).
[18] G. Springholz and K. Wiesauer, Phys. Rev. Lett. **88**, 015507 (2001).
[19] J. Schoiswohl, W. Zheng, S. Surnev, M. G. Ramsey, G. Granozzi, S. Agnoli, and F. P. Netzer, Surf. Sci. **600**, 1099 (2006).
[20] ESRF, 6 rue Jules Horowitz, BP 220, F-38043 Grenoble Cedex, France, www.esrf.eu.
[21] S. Valeri, A. di Bona, and G. C. Gazzadi, Surf. Interface Anal. **21**, 852 (1994).
[22] P. M. Marcus and F. Jona, J. Phys. Chem. Solids **55**, 1513 (1994).
[23] J. P. Hirth and J. Lothe, *Theory of Dislocations* (McGraw-Hill, New York, 1982).
[24] P. Luches, S. D'Addato, S. Valeri, E. Groppo, C. Prestipino, C. Lamberti, and F. Boscherini, Phys. Rev. B **69**, 045412 (2004).
[25] E. Groppo, C. Prestipino, C. Lamberti, P. Luches, C. Giovanardi, and F. Boscherini, J. Phys. Chem. B **107**, 4597 (2003).
[26] S. Valeri, S. Altieri, A. di Bona, C. Giovanardi, and T. S. Moia, Thin Solid Films **400**, 16 (2001).
[27] A. M. Ferrari, S. Casassa, C. Pisani, S. Altieri, A. Rota, and S. Valeri, Surf. Sci. **588**, 160 (2005).
[28] The suppression of the central peaks of the LEED spots might also be related to interference effects induced by the vertical displacements of region in the MgO superstructure cell, as depicted in Fig. 8(e).
[29] L. Giordano, J. Goniakowski, and G. Pacchioni, Phys. Rev. B **67**, 045410 (2003).
[30] C. Giovanardi, A. di Bona, T. S. Moia, S. Valeri, C. Pisani, M. Sgroi, and M. Busso, Surf. Sci. **505**, L209 (2002).
[31] G. Wedler, C. M. Schneider, A. Trampert, and R. Koch, Phys. Rev. Lett. **93**, 236101 (2004).
[32] G. Springholz, N. Frank, and G. Bauer, Appl. Phys. Lett. **64**, 2970 (1994).